

Novel Approach to Improve Electronics Reliability in the Next Generation of US Army Small Unmanned Ground Vehicles Under Complex Vibration Conditions

Ed Habtour · Cholmin Choi · Michael Osterman ·
Abhijit Dasgupta

Submitted: 14 December 2011 / Published online: 10 January 2012
© ASM International 2012

Abstract The functionality of next generation the US Army's platforms, such as the Small Unmanned Ground Vehicles and Small Unmanned Aerial Vehicles, is strongly dependent on the reliability of electronics-rich devices. Thus, the performance and accuracy of these systems will be dependent on the life-cycle of electronics. These electronic systems and the critical components in them experience extremely harsh environments such as shock and vibration. Therefore, it is imperative to identify the failure mechanisms of these components through experimental and virtual failure assessment. One of the key challenges in re-creating life-cycle vibration conditions during design and qualification testing in the lab is the re-creation of simultaneous multi-axial excitation that the product experiences in the field. Instead, the common practice is to use sequential single-axis excitation in different axes or uncontrolled multi-axial vibration on repetitive shock shakers. Consequently, the dominant failure modes in the field are sometimes very difficult to duplicate in a laboratory test. This paper presents the joint effort by the US Army Materiel Systems Analysis Activity (AMSAA) and the Center of Advanced Life Cycle Engineering (CALCE) at the University of Maryland to

develop test methods and analytical models that better capture unforeseen design weaknesses prior to the qualification phase, by better replication of the life-cycle vibration conditions. One approach was to utilize a novel multi-degrees-of-freedom (M-DoF) electrodynamic shaker to ruggedize designs for fatigue damage due to multi-directional random vibration. The merits of vibration testing methods with six-DoF shaker and cost saving associated with such an approach will be addressed in this paper. There is a potential for M-DoF to detect critical design vulnerabilities earlier in the development cycle than has been traditionally possible with existing shaker technologies; and therefore to produce more cost effective, reliable and safe systems for the warfighters.

Keywords Reliability · Physics of failure · Failure mechanisms · Fatigue · Vibration · Multi-axial · Electronics

Introduction

In military applications, electronic devices play a vital role in mission success. These devices which provide control, guidance, communication, and reconnaissance are vital components in modern unmanned vehicular applications. This trend in modern warfare has increased the complexity of electronic equipment, especially in low volume, highly sophisticated, and dense electronic systems. Figures 1 and 2 show the Small Unmanned Ground Vehicles (SUGV) and Small Unmanned Aerial Vehicles (SUAV) [1]. These modern systems take advantage of the remarkable advances made in low cost commercial electronics. It is becoming progressively more beneficial to use such components in military applications for improved computational performance,

Reprinted with permission from *Enabling Sustainable Systems, Proceedings for the MFPT: The Applied Systems Health Management Conference 2011*, Society for Machinery Failure Prevention Technology, 2011, pp. 537–554.

E. Habtour (✉)
US Army Research Laboratory, Vehicle Technology Directorate,
RDRL-VTV, Aberdeen Proving Ground, MD 21005, USA
e-mail: ed.m.habtouri.civ@mail.mil

C. Choi · M. Osterman · A. Dasgupta
Center for Advanced Life Cycle Engineering (CALCE),
University of Maryland, Room 1101, Eng. Lab. Bldg 89,
College Park, MD 20742, USA

on-demand availability, addressing obsolescence, and providing state-of-the-art capabilities. This current movement of using commercial-off-the-shelf (COTS) electronics and devices for military applications has led to concerns about their reliability in harsh battlefield environments. Typically, these types of systems are subjected to various complex loadings, including shock and vibration, during their life-cycle. These loads may impose significant stresses on the PCB substrate, component packages, leads and solder joints [1]. These stresses can be due to a combination of bending moments in the PCB and/or inertias of components. They may lead to several failures such as delamination in the PCB, solder joint fatigue, lead fracture or structural damage to components.

When conducting PoF analysis of electronic systems, the large variety of package types is perhaps one of the main challenges to consider, since failure may occur due to one of several failure drivers. One of the most frequent failures in electronics is the package to board interconnect in heavy components with large center of mass (CM) and low-profile surface mount packages (SMT). The failure in heavy components with large CM can be predominantly due to inertial loads. While in light low-profile SMT



Fig. 1 SUGV



Fig. 2 SUAV

packages, the dominant stress source can be due to board deflection. Both of these failure drivers may compete in heavy and large electronic components such as inductors and transformers. Depending on the architecture of these components, they can also significantly alter the local vibration response. It is common to increase the board stiffness to reduce the overall response of the PCB. However, increasing the board stiffness may increase local bending moments.

The current available vibration fatigue life prediction methods for large/heavy components force reliability engineers to use one of two extremes. One method is to construct a detailed 3D FEA. This approach may be impractical when dealing with large circuit card assemblies (CCA) containing many components, each with multiple leads and solder joints. Further, these methods can be computationally expensive and their accuracy may be compromised due to assumptions in material properties and support conditions. The other extreme is to use simple empirical equations. Probably the best-known empirical method to estimate component life under vibration is Steinberg's model [2]. However, these models are also limited to a defined set of boundary conditions and package structures. Therefore, they cannot be the only design tool to evaluate new products or emerging technologies with a high level of confidence.

This paper is concerned with a rapid analytical technique for analyzing heavy/large components that can provide an engineer high fidelity assessment while reducing the computational time. A PoF approach was developed that may improve the reliability assessment of CCAs containing large/heavy components. This approach is a hybrid-method that combines 2D and 3D FEA where the mechanical and inertial properties of the components at the local level are taken into consideration. These properties may be used to extract an accurate natural frequency value for the CCA. Nonetheless, this approach may not eliminate the need to address the components inertial effects.

Physics of Failure Approach

Simplified Single-Degree-of-Freedom Approach

As mentioned above one of the best known simplified models for analysis of PCB vibration fatigue is Steinberg's model [2]. Steinberg's model defines a critical maximum vibration induced displacement for components as [2]:

$$d = \frac{0.00022B}{Chr\sqrt{L}} \quad (\text{Eq 1})$$

where B is the length of the PCB edge parallel to the component located at the center of the board in units of

inches. L and h are the length of the component and the thickness of the PCB in inches, respectively. C is a constant coefficient which depends on the component type and r is the relative position factor of the component relative to the PCB. The Steinberg model assumes a dynamic single-amplitude displacement for the PCB. This model is valid only for single-degree-of-freedom (SDOF) systems. The out-of-plane root-mean-square (rms) displacement is calculated as follows [2]:

$$Z_{rms} = \frac{9.8G_{rms}}{f_n^2} \tag{Eq 2}$$

where f_n is the natural frequency and G_{rms} is the root-mean-square output acceleration. The G_{rms} can be estimated using Miles' equation:

$$G_{rms} = \sqrt{\frac{\pi P f_n Q}{2}}, \quad \text{where } Q = \sqrt{f_n} \tag{Eq 3}$$

where P is the input Power Spectral Density (PSD) and Q is the transmissibility. Steinberg states when the dynamic single-amplitude displacement at the center of the PCB is limited to the critical value d , the component is expected to achieve a fatigue life of 20 million stress reversals in a random vibration environment and 10 million stress reversals under sinusoidal vibration. One must be cautious when using this model since Steinberg's empirical approach is based on a specific experimental data set from a particular collection of specimen architectures and boundary conditions. Thus, this empirical approach may be more accurate when applied to PCBs assembled in exactly the same manner. The drawback of his model is that it cannot be used outside the range and configuration of the assembly used in the derivation of the model. It cannot be used to evaluate new products or emerging technologies with high confidence. Nonetheless, this approach may help designers obtain a rough estimate of the acceleration factors for accelerated vibration durability tests and for comparing the relative dynamic robustness of competing designs.

Electronically dense military platforms have to endure severe and complex dynamical loading conditions during

the life-cycle, resulting in high-cycle fatigue. For complex structure and dynamic loading Steinberg's model alone may not be an adequate approach for assessing the survivability of military devices.

In this study a $127 \times 101.6 \text{ mm}^2$ PCB with six large/heavy inductors was designed, as shown in Fig. 3. The inductor geometry is shown in Fig. 4.

The PCB was assumed to be fixed (clamped) along the short edges of the board, as illustrated in Fig. 3 with the red dots. The objective is to evaluate 2D and 3D FEA approaches to assess the reliability of large electronic components. A more cost effective approach combining 2D and 3D FEA was developed to extract the natural frequency of the PCB and more accurately determine the maximum deflection, curvature, and stress. The goal is to evaluate whether this approach can detect critical failure risks early in the development cycle. The modeling also provides effective guidance for future vibration testing using a multi-degree-of-freedom (M-DoF) electrodynamic (ED) shaker. The test results will be used in the future to evaluate the accuracy of this modeling approach and to assess the effect of the local inertia of large/heavy components on the fatigue life of interconnects.

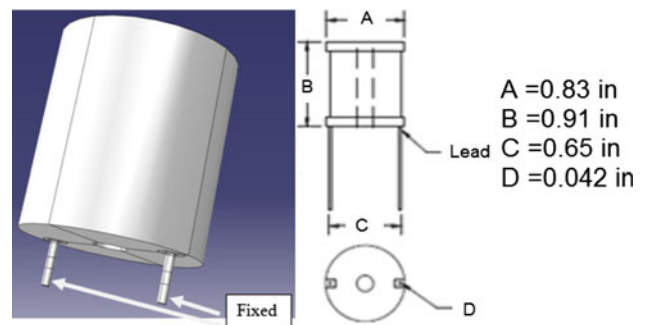
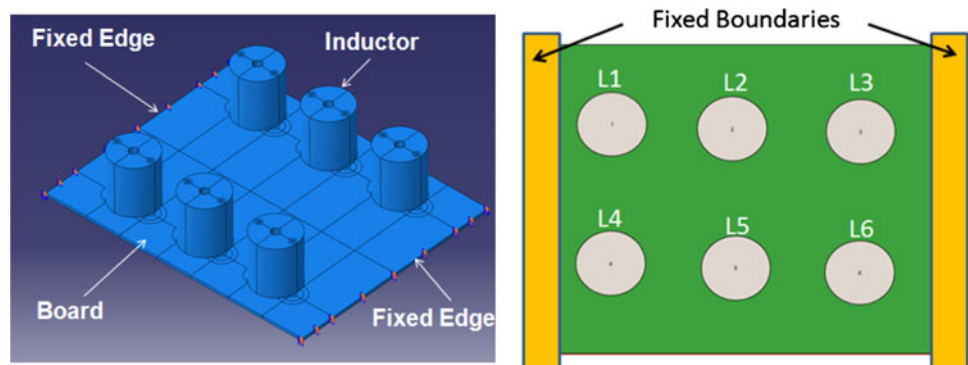


Fig. 4 Large inductor used in this study

Fig. 3 CAD model of PCB with large components



Two-Dimensional Approach

A more detailed approach than the Steinberg model when conducting PoF analysis is a simplified 2D (plate or shell) FEA of a PCB. The mass of the components are “smeared” over their PCB footprints to reduce computational time and cost. This method was developed by Pitarresi and Primavera where they performed experimental and FEA modeling work to characterize the natural frequencies, mode shape, and transmissibility at the board level [3]. Later, they used the simple plate vibration models, using the property smearing approaches, as well as detailed finite element modeling. In the case where the local inertias are significant, a traditional 3D FEA might be necessary. Transforming a 3D PCB model in Fig. 3 to 2D FEA using the smeared technique is shown in Fig. 5. The PCB was discretized into rectangular shell elements, as shown in Fig. 5. The individual elements were defined by four nodes. Typically in traditional FEA, the shell element nodes in a continuum structure have six-DoF. For PCB PoF analysis, the number of degrees of freedom was reduced to three plate DOFs, which includes one out-of-plane displacement, u_z , and two rotations about the two orthogonal axes in the plane of the board. The displacement of each node is driven by the element’s stiffness matrix. The element stiffness matrix is a function of the element geometry and the constitutive material properties. Because PCBs have multilayer composite construction, laminated plate theory was used to calculate the element stiffness matrix. The layers’ geometric and material properties were designed symmetrically about the middle surface of the board. Therefore, the bending-extension coupling effect was not a cause for concern and the extension and the coupling matrixes were eliminated [4]. This led to a simplified plate equation with the bending stiffness only:

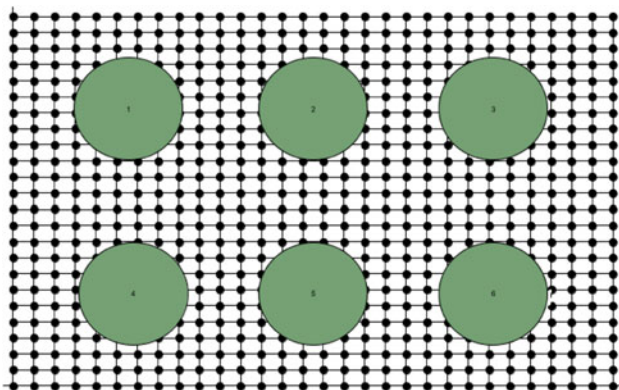


Fig. 5 2D FEA of PWB and inductors, using smearing method

$$\begin{Bmatrix} M_x \\ M_y \\ M_{xy} \end{Bmatrix} = \begin{bmatrix} D_{11} & D_{12} & 0 \\ D_{12} & D_{22} & 0 \\ 0 & 0 & D_{33} \end{bmatrix} \begin{Bmatrix} \kappa_{xx} \\ \kappa_{yy} \\ 2\kappa_{xy} \end{Bmatrix} \tag{Eq 4}$$

where $\{M\}$ and $\{\kappa\}$ are the moment resultant and board curvature vectors. The flexural (or bending) rigidity matrix, $[D]$, is the measure of how easily the board bends. $[D]$ can be calculated as follows:

$$D_{ij} = \frac{1}{3} \sum_{k=1}^n Q_{ij}^k (h_k^3 - h_{k-1}^3), \quad \text{for } i, j = 1, 2, 3 \tag{Eq 5}$$

where i and j coincide with the natural axes of the material and n is the number of layers in the PCB. The distance of the outermost fiber of the k th layer from the mid-surface of the plate is h_k . Q_{ij}^k is the material stiffness matrix for the material in layer k [4] for additional information on how to calculate Q_{ij} . For a uniform, symmetrical, homogeneous composite construction the board rigidity, $D_{11} = D_{22} = D$, may be approximated as:

$$D = \frac{Et^3}{12(1 - \nu^2)} \tag{Eq 6}$$

where E is the elastic modulus, t is the board thickness and ν is the Poisson’s ratio. After obtaining the $[D]$ matrix, the board curvature can be calculated from the simplified plate Eq 4. The smeared technique was then implemented using 2D shell elements.

The smeared technique includes the mass of the board and components by simply increasing the mass of the shell element under the footprint of each component. However, the component stiffness is not included in this simplified smearing approach. The first mode natural frequency for this board, using this smearing approach, is 108 Hz.

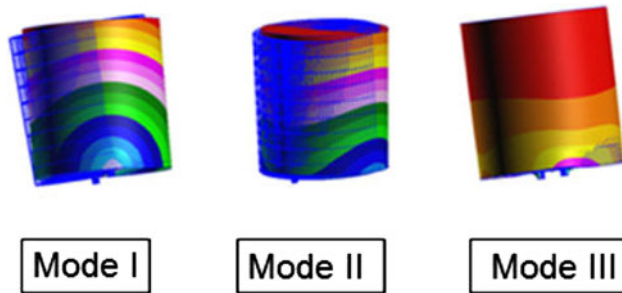
However, for large/heavy through-hole components, some 2D codes may approximately include the stiffening effect of the components. In this approach, the mass and stiffening effects are included by locally increasing the PCB’s density and Young’s modulus, respectively. Unfortunately, such an approach does not address the inertias and radius of gyration of large components with high standoff. These effects can cause additional stresses in the leads and interconnects and a traditional 3D FEA might be necessary to analyze this effect.

Three-Dimensional Approach

In this study, modal analyses were first conducted on just the inductor with various standoff heights as shown in Table 1. In this task, the component leads were assumed to be “fixed” at the interface with the PWB, as shown in Fig. 4. As expected the modal frequency dropped as the standoff height increased, due to the component’s significant inertia. Resulting mode shapes are shown in Fig. 6.

Table 1 Inductor modal response for various standoff heights

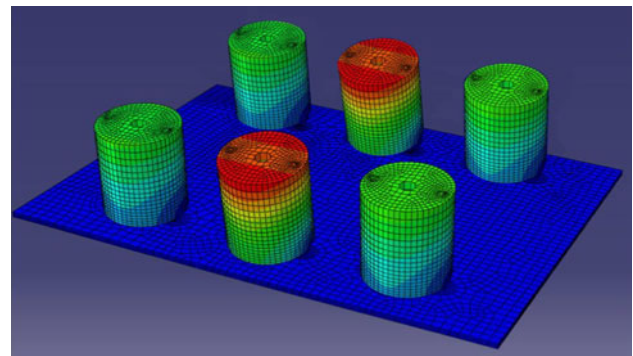
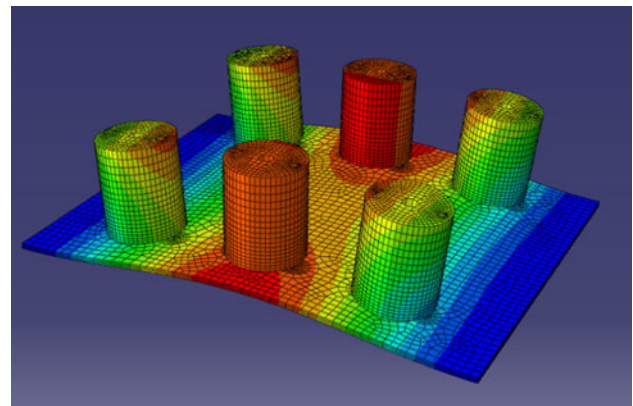
Standoff height, mm	Mode I, Hz	Mode II, Hz	Mode III, Hz
0.5	108	1733	3266
1.0	102	1657	3161
1.5	98	1560	2682
2.0	94	1430	2200

**Fig. 6** Inductor modal shapes when fixed at leads

This additional motion will clearly have a significant impact on the stresses induced in the interconnects but these effects are typically neglected in the smeared properties technique.

To more accurately model the system, a 3D model of the board with attached inductors was constructed and analyzed. In this analysis, the modal frequencies of the inductors dropped significantly because of the compliance of the PWB attached to the lead foot. The first mode response of the middle inductors is depicted in Fig. 7. The inductor standoff height in this analysis was 2.0 mm and the maximum response occurred in the components located at the middle of the PCB. The frequency for the first vibration mode for the middle components and the components closer to the fixed edges was approximately 71 Hz, which is approximately 20% lower than the frequency for a rigidly clamped lead foot. The PCB's first vibration mode was 159 Hz, which was about 45% higher than that predicted by the smeared 2D model, because of the additional stiffening effect of the components. The first mode shape of the PCB is shown in Fig. 8.

In typical vibration fatigue analysis, the PCB is treated as a thin plate. Therefore, many researchers reasoned that the PCB's natural frequency is dependent upon the geometry and the material of the board and not necessarily on the components [5]. This might be valid for micro-electronic components with low mass and low standoff, where the drop in natural frequency due to the added mass of the components is compensated for by the increase in the natural frequency due to the local increase in stiffness from component mounting. However, for large/heavy components the scheme may not be applicable since the increase

**Fig. 7** Middle inductor's first modal response**Fig. 8** PCB first modal response

in the component mass and the leads stiffness might not cancel each other. The first vibration mode for the PCB described above when neglecting both the inertial and stiffness effects of the components was approximately 310 Hz. Clearly, neglecting the mass and stiffness effects of the inductor over estimated the natural frequency of the PCB. If the mass effect of the components was included only in this particular PCB, the natural frequency was 108 Hz, while inclusion of the stiffening effects also, (using the 3D global FEA model) increases the frequency to 159 Hz.

Combined Two- and Three-Dimensional Approach

In this study the simplicity of the global 2D FEA was combined with a more detailed local 3D FEA. The advantages of this approach are significant cost and time reduction without resorting to full 3D FEA. In this approach, the local 3D FEA model was considered first. Based on the knowledge of the effective moment–curvature relationship near the component of interest, a local effective stiffness was determined. The warpage was evaluated by simply applying a local unit load to the local model, as shown in Fig. 9. This caused the PCB to

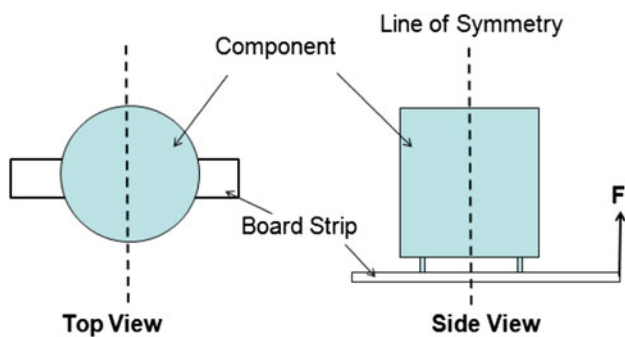


Fig. 9 Local FEA model

experience small dynamic deflection or warpage. The local deformation was modeled with two radii of curvature. This was accomplished through the use of Kirchhoff-plate moment–curvature equations (found in several structural textbooks), where the local radii of curvature and the local applied bending moments are related as follows:

$$\begin{aligned} \begin{Bmatrix} M_{xx} \\ M_{yy} \\ M_{xy} \end{Bmatrix} &= \begin{bmatrix} D_{11} & D_{12} & 0 \\ D_{12} & D_{22} & 0 \\ 0 & 0 & D_{33} \end{bmatrix} \begin{Bmatrix} \kappa_{xx} \\ \kappa_{yy} \\ 2\kappa_{xy} \end{Bmatrix} \\ \begin{Bmatrix} M_x \\ M_y \\ M_{xy} \end{Bmatrix} &= \frac{h^3}{12} \begin{bmatrix} E_{11} & E_{12} & 0 \\ E_{12} & E_{22} & 0 \\ 0 & 0 & E_{33} \end{bmatrix} \begin{Bmatrix} \kappa_{xx} \\ \kappa_{yy} \\ 2\kappa_{xy} \end{Bmatrix} \end{aligned} \tag{Eq 7}$$

where $D_{ij} = E_{ij}h^3/12$ for $i, j = 1, 2, 3$. Assuming an isotropic Poisson’s ratio for simplicity, the local effective stiffness due to the presence of the component can be calculated as follows:

$$D_{11} = \frac{M_x - \nu M_y}{\kappa_x(1 - \nu^2)} \tag{Eq 8}$$

Similarly,

$$D_{22} = \frac{M_y - \nu M_x}{\kappa_y(1 - \nu^2)} \tag{Eq 9}$$

The curvature can be calculated from the PWB deflection of the local 3D FEA model, by the relationship below which can be obtained in any calculus book:

$$\kappa_x = \frac{\frac{d^2y}{dx^2}}{\left(1 + \frac{d^2y}{dx^2}\right)^{3/2}} \tag{Eq 10}$$

where the elastic deflected curve was expressed mathematically as $y = f(x)$. The component was assumed to remain rigid and all the deformation was assumed to occur in the PWB and the leads. This assumption was made in the local model to make the displacement calculation more manageable.

The global 2D FEA model was constructed in the manner discussed above. However, the local flexural rigidity matrix, [D], was replaced at the footprint of each

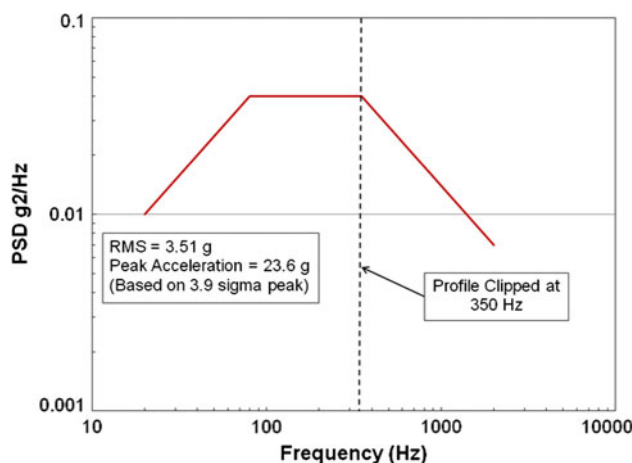


Fig. 10 NAVMAT P9492 ASD/PSD

component, with the ones calculated from the local 3D FEA model. The first vibration mode was then obtained from the 2D global model, which was 160 Hz. This value was close to that obtained from the full 3D FEA model discussed above. Therefore, one may use a combined two–three-dimensional approach to reach similar results to a full 3D FEA with the advantages of less computational time and cost reduction.

Although this approach may improve the prediction of the first mode of the CCA, it does not take into account the inertial effect of the large components. Therefore, a spectral response analysis was conducted using the global 3D FEA model, for the NAVMAT P9492 Acceleration/Power Spectral Density (ASD/PSD) profile (Fig. 10). The profile was clipped at 350 Hz, meaning the analysis was performed for 0–350 Hz range. This was done to study the first two modes of the assembly. A base motion excitation was used at the boundary for each in-plane direction (x and y directions) and out-of-plane (z direction) individually. The direction of the excitations and responses are shown in Fig. 11. This analysis was followed by combined excitation in all directions: x, y and z . The PSD acceleration responses are given in Fig. 12. It can be seen from Fig. 13 that the center component experienced the highest excitation in the in-plane y direction as well as a slightly lower excitation in the out-of-plane direction at the first mode frequency of the component, 70 Hz. Another interesting observation is the component is excited in the out-of-plane direction at the first frequency mode of the board. In terms of the PWB, the dominant mode is the first mode of the board, as expected. Nonetheless there were dynamic effects due to the excitation in the y direction that caused an acceleration peak in the PWB at the component natural frequency, 70 Hz. This peak is generated by the component’s high inertia which produces a rocking motion as shown in Fig. 11.

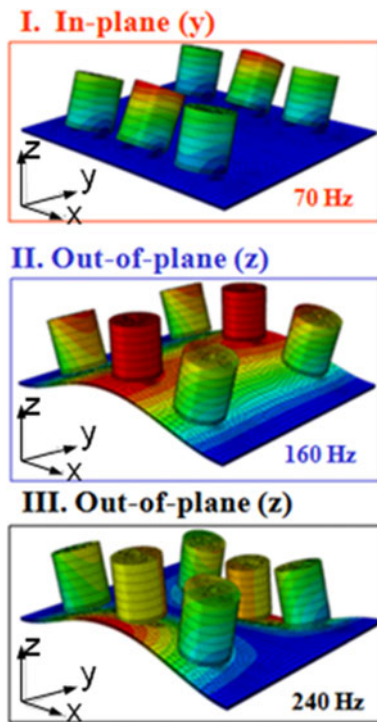


Fig. 11 Response analysis

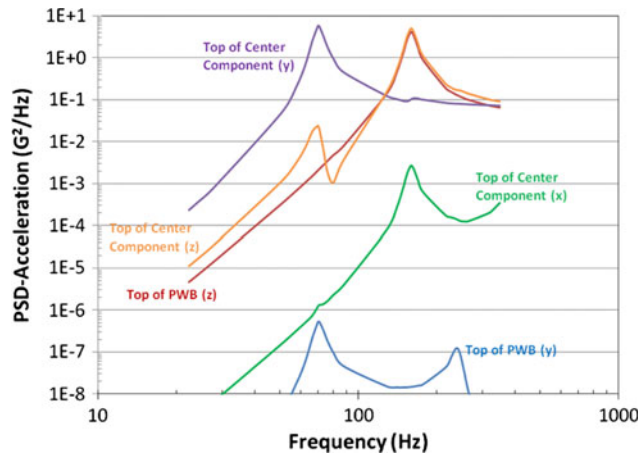


Fig. 12 Spectral response analysis

Finally, the PSD of the analyzed lead stress due to the combined dynamic loading is shown in Fig. 13. The maximum stresses were located at the leads of the center components, as illustrated in Fig. 14. The stresses shown in this figure were the z-component stresses. This stress component represents the bending stresses in the leads, caused by combination of inertial loads and the board deflection. Because of the board architecture and the components' inertial effect there might be alteration in the local vibration response. As mentioned above, it is a common practice to increase the board stiffness under the

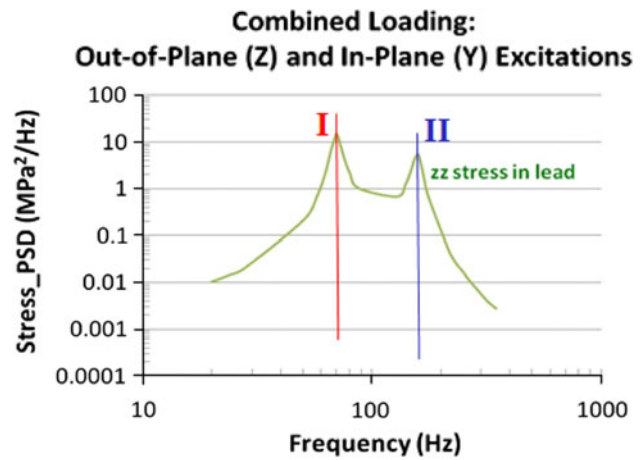


Fig. 13 Stress due to combined loading

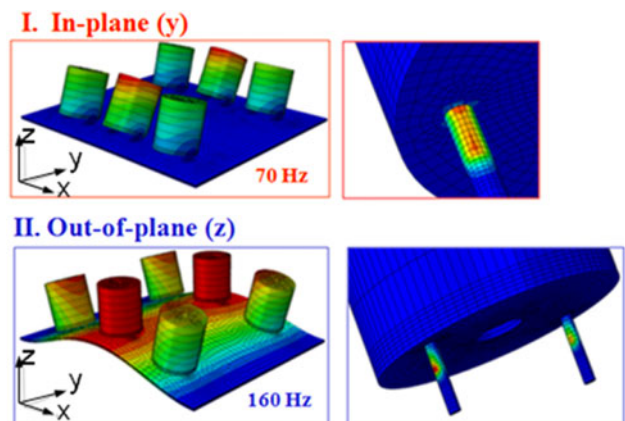


Fig. 14 Maximum stresses at component leads

footprint of the component, to reduce the overall response of the PCB but this may increase local bending moments and stresses in the PWB.

Clearly, the modified smeared technique may address the overall stiffness of the CCA and produce an accurate PWB first mode frequency, however, it doesn't tackle failure in heavy components. Therefore, the best practice is to conduct a M-DoF accelerated vibration test to assess the actual damage accumulation rates in the components, leads and PWB; followed by full 3D FEA modeling to generate acceleration factors that can be used to extrapolate the test results to various life-cycle conditions and mission profiles. In practice, engineers often use one of these two approaches (i.e. modeling or testing) to qualify the product. The next section addresses the testing methodology.

Testing Approach

When considering PoF of electronics in ground vehicles, there are two types of motion that should be considered.

One motion is the induced curvature or bending in the PCB as the assembly moves in a vibratory manner (global motion). The other motion is the movement of individual components with respect to the PCB due to the compliance of the components' attachment (local motion). To accurately assess how the excitations are transmitted from the vehicle to the electronic component level, some researchers have suggested modeling the dynamic response of the vehicle subsystems. This approach, however, can be an arduous task [6]. The main reason for this lies in the fact that the vehicle chassis and body are complex systems. The reaction forces and vibration velocities depend not only on the strength of excitation within the chassis but also on the coupling of the chassis and the subsystems.

Thus, one has no choice but to count on engineering judgment in estimating the boundary conditions and system inputs. A more practical approach perhaps is using experimental Frequency Response Function (FRF) data to represent the vehicle then combine it with the FEA models of the subassembly.

Two approaches utilized in this study for M-DoF testing are based on a Repetitive Shock (RS) shaker and a M-DoF ED shaker. A typical RS shaker, as depicted in Fig. 15, utilizes a collection of pneumatic actuators to impart impact energy to a specially designed vibration table that transmits the resulting multiaxial vibration energy to test specimens mounted on the table. The RS shaker is often used in the industry to identify marginal designs and design weaknesses that, due to statistical variability, would eventually result in premature field failures when production quantities of the product are exposed to life-cycle conditions. This method relies on the use of elevated stresses to determine the operating and destruct limits of the design.

The test is performed in a chamber which typically has a broad spectrum of vibration energy from 10 to 5,000 Hz and runs from 1 to $150G_{rms}$.

The RS testing typically does not provide quantitative information of acceleration factors for precipitated failure mechanisms, due to two major limitations [7]. First, the only input that can be controlled during vibration testing is the G_{rms} in the vertical direction (or Z direction). Thus, it is impossible to control the shape of the PSD profile, as shown in Fig. 16 [7]. Secondly, since the chamber employs pneumatically driven hammers, it is impossible to independently control each DoF. Furthermore, Center of Advanced Life Cycle Engineering (CALCE) has confirmed that the coherence between the axes is nonexistent, as shown in Fig. 17 [7]. Thus, it is difficult to determine the acceleration of failure and/or the DoF that instigates the most damage to the components. Therefore, a quantitative relationship between performance in the field and performance in the test is difficult to establish.

Due to these limitations of RS shakers in M-DoF vibration testing, this team is investigating the possibility of utilizing multiaxial electrodynamic (M-DoF ED) shakers. The objective is to study the differences in failure modes and fatigue life for simultaneous multi-axis excitation versus single-axis excitation.

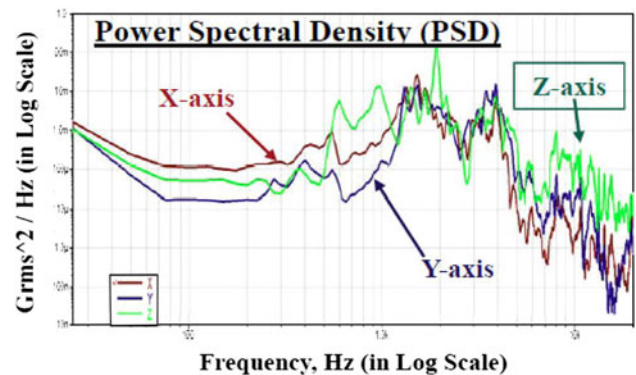


Fig. 16 PSD in RS shaker [7]



Fig. 15 Typical RS shaker architecture

The M-DoF ED shaker used in this study consists of 12 electrodynamic actuators; 4 for each of the three orthogonal excitation axes. Eight are in-plane and four out-of-plane (underneath the shaker table), as shown in Fig. 18. The 12 ED shakers are mechanically coupled to the table via self-aligning hydrodynamically lubricated bearings. The four actuators in each axis can be run in-phase or out-of-phase to produce translation in that axis or rotation about transverse axes. This architecture allows the shaker to produce a true M-DoF vibration environment. The actuators can exert up to 200 lbf force per axis with max translation of ± 0.25 inches and max rotation of $\pm 5^\circ$. The excitation limit is up to 30 Gs with 0–3000 Hz for a 10 lb payload. Unlike other testing methodologies, multiaxial ED shakers provide a more controlled simultaneous loading along different axes of a test specimen, thus, allowing controlled exploration of cross-axis interactions that could not be easily explored with single-axis excitation or with RS shakers. The input PSDs and coherences can be controlled for all axes, as demonstrated by CALCE (Fig. 19)

[7]. Figure 19 shows excellent control of the shape of the excitation PSD profile. CALCE has also shown that the coherence between the axes is excellent as shown in Fig. 20. Therefore, it is possible to identify the most dominant failure mechanisms or the DoF that instigates the most damage to the components.

The M-DoF ED shaker at CALCE will be utilized to excite the test PWB with large insertion-mount components, to levels seen on the battlefield, such as the NAVMAT P9492 PSD profile. The FRF experimental data will be combined with the FEA model where the interconnect fatigue results would be extracted with the aid of FEA.

This approach may help in establishing a quantitative relationship between performance in the battlefield and performance in the test. It may also produce a modified smeared modeling approach that addresses inertial effects of large/heavy components without the need to resort to a fully three-dimensional detailed FEA model.

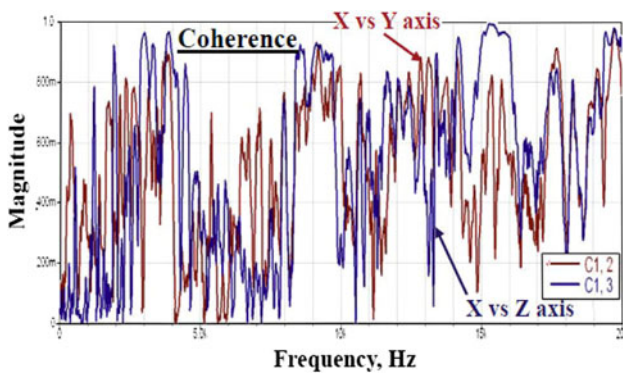


Fig. 17 Cross-axis coherence in RS shaker [7]

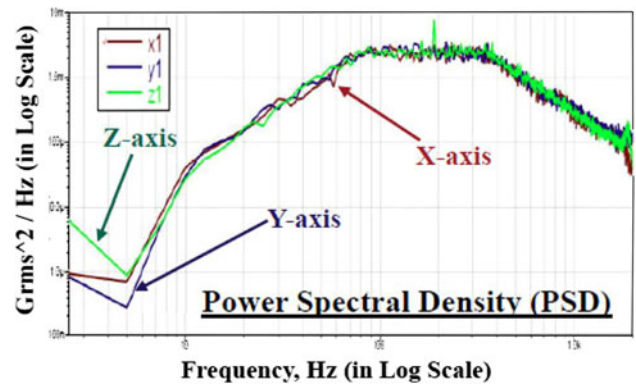
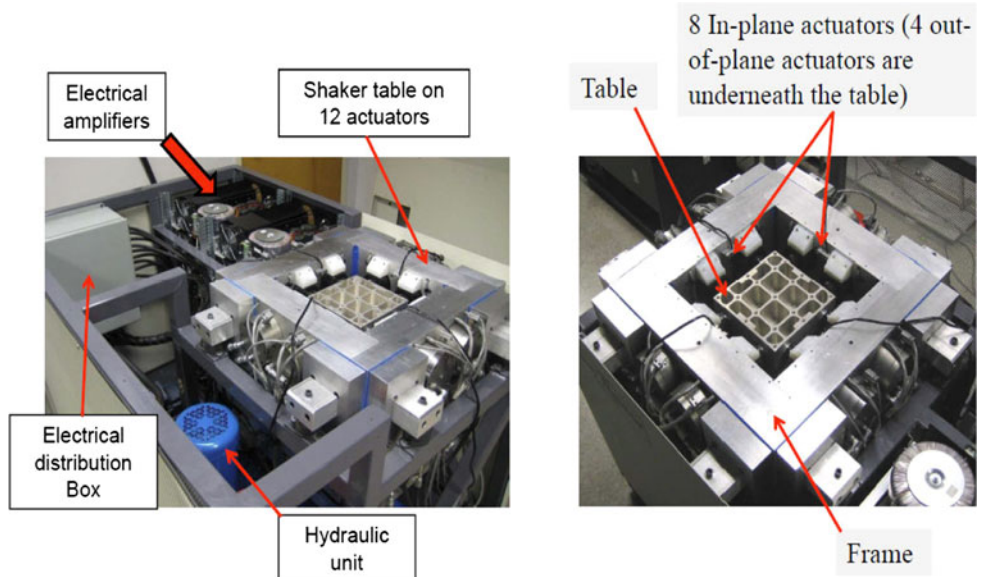


Fig. 19 PSD in M-DoF ED shaker [7]

Fig. 18 Multiaxial six-DoF ED shaker



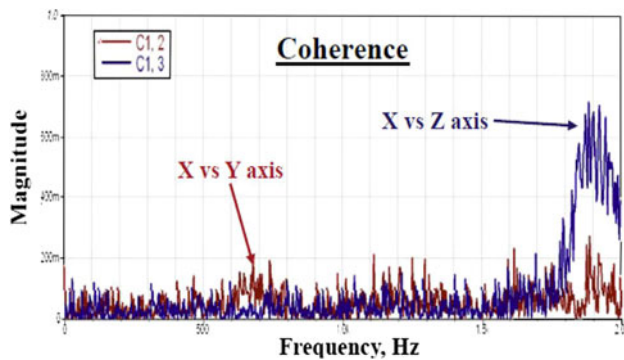


Fig. 20 Coherence in M-DoF ED shaker [7]

Future Work

Vibration durability tests will be conducted on the M-DoF ED shaker for various excitation orientations: (i) out-of-plane; (ii) in-plane; (iii) simultaneous in-plane and out-of-plane; and (iv) sequential in-plane and out-of-plane excitations. Subsequently, destructive physical analysis of failed specimens will be conducted. The final step will be to develop a PoF modeling approach for vibration durability under random, multi-modal and M-DoF excitations. The natural frequencies and mode shapes will be extracted from FEA modal analysis and compared with testing results. For this step, test specimens will be fabricated (PCB with heavy through-hole inductors) to conduct a M-DoF vibration durability test on the M-DoF shaker. Additionally, FEA simulation will be carried out to characterize the dynamic response of the test CCA. Response characterization will mainly include dynamic strain history collected on the test vehicle. Corresponding FEA will be conducted and calibrated, based on the experimental results. The characteristic flexural strain at different locations on the test board can then be either measured with strain gages or estimated from the FEA model, under different excitation levels. These strain time histories are then used to construct strain range distribution functions of the PCB, based on cycle counting.

Outcomes

As discussed above, the fatigue damage in the interconnects can be due to a combination of flexural deformations

in PCBs and/or due to inertial forces caused by the mass of large/heavy components with high standoff. When conducting electronics PoF, a hybrid two/three-dimensional FEA approach may provide natural frequency results closer to full 3D FEA while reducing cost and computational time. However, failures predominantly due to inertial loads may require full 3D FEA, testing, or both.

It is essential to understand the structural characteristics of large/heavy components in electronics devices in order to correlate the defects with the dynamic responses. As mentioned above, the main challenge in electronics packaging is the prediction of the reliability and lifetime of the critical components. Therefore, it is imperative to identify the failure mechanisms of the components through experimental analysis. However, the experimental approach has to emulate the real world operational conditions, which includes simulating M-DoF dynamic loads. This involves experimentally measuring the transient in-plane and out-of-plane displacement responses which can be accomplished with the aid of a multiaxial shaker.

This investigation will be utilized to enhance and improve existing standards for dealing with complex dynamic loading in electronics. It will also aid AMSAA in establishing a quantitative relationship between performance in the battlefield and performance in the test. It may also provide a means to validate and improve existing physics of failure models.

References

1. Erwin, S.I.: In Damage Control Mode, Army Builds Future Network of Combat Brigades. National Defense (2010)
2. Steinberg, D.: Vibration Analysis for Electronic Equipment, 3rd edn. Wiley Inter-Science, New York (2000)
3. Pitarresi, J., Primavera, A.: Comparison of Vibration Modeling Techniques for Printed Circuit Cards. ASME J. Electron. Packag. **114**, 378–383 (1991)
4. Jones, R.M.: Mechanics of Composite Materials, 2nd edn. Taylor and Francis Group, New York (1999)
5. Barker, D.B., Chen, Y.S.: Modeling vibration restraint of wedge lock card guides. In: ASME Annual Meeting, 92-WA/EEP-16, Anaheim, CA, November 1992
6. Li, R.S.: A methodology for fatigue prediction of electronic components under random vibration load. J. Electron. Packag. ASME **123**, 394–400 (2001)
7. Choi, C., Al-Bassiyouni, M., Dasgupta, A., Osterman, M.: PoF issues in multi-DoF vibration testing: ED shakers and RS shakers. In: IEEE ASTR09 Workshop, New Jersey, October 2009